Phosphorus-31 Solid-State NMR Studies of Homonuclear Spin Pairs in Molybdenum Phosphine Complexes: Single-Crystal, Dipolar-Chemical Shift, Rotational-Resonance, and 2D Spin−Echo NMR Experiments

Klaus Eichele, Gabriel C. Ossenkamp, Roderick E. Wasylishen,* and T. Stanley Cameron

Department of Chemistry, Dalhousie University, Halifax, Nova Scotia, Canada B3H 4J3

Received June 4, 1998

Several solid-state NMR techniques have been employed to characterize phosphorus chemical shift tensors and $^{31}P-^{31}P$ spin−spin coupling interactions for bisphosphine molybdenum complexes where only one phosphorus of the bisphosphine ligand is coordinated to the metal. The bisphosphine ligand of each complex was either tetraphenyldiphosphine, tpdp, or bis(diphenylphosphino)methane, dppm. For one compound, $(OC)_5Mo(\eta^1$-dppm), single crystals were examined by ^{31}P NMR and X-ray diffraction. For the metal-bound phosphorus, the most shielded direction of the chemical shift tensor is near the Mo−P bond axis. For the non-coordinated phosphorus, the most shielded direction is oriented in the direction of the formal electron lone pair on phosphorus. For the other compounds, stationary powder samples were examined using dipolar-chemical shift and 2D spin−echo techniques. Powder samples were also examined under slow magic-angle spinning, variable-angle spinning, and rotational-resonance conditions. Analysis of these ^{31}P NMR spectra suggested chemical shift tensor orientations analogous to those measured for the single crystal; however, in the case of powders only the relative orientations of the two chemical shift tensors with respect to the P−P axis can be determined. Our investigations indicate that spectra from powder samples should be analyzed at two or more applied magnetic fields. The 2D spin−echo experiment proved to be invaluable for obtaining the effective dipolar P,P coupling constant, *R*, and the relative signs of *R* and the indirect spin−spin coupling constant, *J*. Values of $^nJ(^{31}P,^{31}P)$ measured in the solid state often differ significantly from the conformationally averaged values obtained in solution. The tpdp derivatives appear to have a reduced *R*, whereas for the dppm systems, *R* agrees very well with the value calculated from the known P,P separations.

Introduction

Transition metal centers coordinated by phosphine ligands are important precursors, intermediates, or products in organometallic chemistry. Polydentate phosphines, in particular, offer several advantages compared to monophosphine complexes, such as increased nucleophilicity at the metal center, better control of stereochemistry, and slower, more controlled intra- and intermolecular exchange reactions.[1] An important feature of metal phosphine complexes is that their kinetics and structure can be monitored by ^{31}P NMR spectroscopy. The potential of ^{31}P NMR in characterizing these systems in solution has been amply demonstrated.[2] Many phosphine transition metal complexes have also been studied in the solid state by high-resolution ^{31}P magic-angle spinning (MAS) NMR.[3] While isotropic phosphorus chemical shifts are readily obtained from such studies, considerably less information is available on phosphorus chemical shift tensors in these systems.[4]

The purpose of the present study is to characterize the phosphorus chemical shift tensors of several molybdenum bisphosphine complexes (see Chart 1), where only one phosphorus atom of the ligand, R_2P-$(CH_2)_n$-PR_2, is coordinated to the metal. The results obtained for these systems will be important in improving our understanding of coordination shifts, δ(complex) − δ(ligand). This research was also stimulated by recent progress in calculating chemical shielding tensors using *ab initio* methods, which are now beginning to produce promising results for systems containing transition metals.[5] An additional motivation for this study was to develop a protocol

* Address correspondence to this author. Tel.: +1 (902) 494-2564. Fax: +1 (902) 494-1310. E-mail: Roderick.Wasylishen@Dal.Ca.

(1) Cotton, F. A.; Hong, B. *Progr. Inorg. Chem.* **1992**, *40*, 179.

(2) (a) Pregosin, P. S.; Kunz, R. W. In *NMR, Basic Principles and Progress*; Diehl, P., Fluck, E., Kosfeld, R., Eds.; Springer-Verlag: Berlin, 1979; Vol. 16. (b) *Phosphorus-31 NMR Spectroscopy in Stereochemical Analysis: Organic Compounds and Metal Complexes*; Verkade, J. G., Quin, L. D., Eds.; Methods in Stereochemical Analysis 8; VCH Publishers, Inc.: Deerfield Beach, FL, 1987. (c) Dixon, K. R. In *Multinuclear NMR*; Mason, J., Ed.; Plenum Press: New York, 1987; p 369. (d) *Phosphorus-31 NMR Spectral Properties in Compound Characterization and Structural Analysis*; Quin, L. D., Verkade, J. G., Eds.; VCH Publishers, Inc.: New York, 1994.

(3) (a) Davies, J. A.; Dutremez, S. *Coord. Chem. Rev.* **1992**, *114*, 61. (b) Colin, C. A. *Solid State NMR for Chemists*; C.F.C. Press: Guelph, ON, 1983.

(4) (a) Duncan, T. M. *A Compilation of Chemical Shift Anisotropies*; The Farragut Press: Chicago, 1990. (b) Jameson, C. J. In *A Specialist Periodical Report: Nuclear Magnetic Resonance*; Webb, G. A., Ed.; The Royal Society of Chemistry.

(5) (a) Nakatsuji, H.; Hada, M.; Kaneko, H.; Ballard, C. C. *Chem. Phys. Lett.* **1996**, *255*, 195. (b) Kaupp, M.; Malkin, V. G.; Malkina, O. L.; Salahub, D. R. *Chem. Eur. J.* **1996**, *2*, 24. (c) Kaupp, M. *Chem. Ber.* **1996**, *129*, 535. (d) Ruiz-Morales, Y.; Schreckenbach, G.; Ziegler, T. *Organometallics* **1996**, *15*, 3920. (e) Schreckenbach, G.; Ziegler, T. *Int. J. Quantum Chem.* **1997**, *61*, 899. (f) Bühl, M. *Chem. Phys. Lett.* **1997**, *267*, 251. (g) Chan, J. C. C.; Wilson, P. J.; Au-Yeung, S. C. F.; Webb, G. A. *J. Phys. Chem. A* **1997**, *101*, 4196. (h) Godbout, N.; Oldfield, E. *J. Am. Chem. Soc.* **1997**, *119*, 8065. (i) Havlin, R.; McMahon, M.; Srinivasan, R.; Le, H.; Oldfield, E. *J. Phys. Chem. A* **1997**, *101*, 8908. (j) Bernard, G. M.; Wu, G.; Wasylishen, R. E. *J. Phys. Chem. A* **1998**, *102*, 3184. (k) Schreckenbach, G.; Ziegler, T. *Theor. Chem. Acc.* **1998**, *99*, 71.

10.1021/ic9806232 CCC: $18.00
Published on Web 01/28/1999

Chart 1

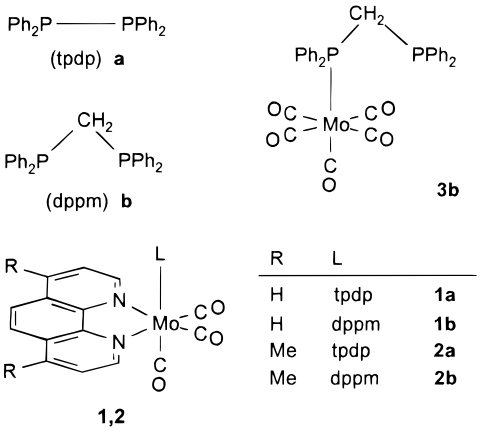

for analyzing NMR spectra of homonuclear spin pairs in the solid state. Whereas only the chemical shift difference and the indirect spin−spin coupling constant are required to describe a two-spin system in isotropic solution NMR, the situation in solids is more complex. In principle, one requires three principal components and three angles to characterize each chemical shift tensor. Also required are the direct dipole−dipole and indirect spin−spin coupling tensors. Here, we examine the utility of the dipolar-chemical shift NMR technique, slow MAS, variable-angle spinning (VAS), 2D spin−echo NMR and rotational-resonance techniques. While the rotational-resonance technique has been used extensively for determining dipolar coupling constants in biological systems, we are unaware of applications of this technique to organometallic systems.

Experimental Section

Sample Preparation. Tetraphenyldiphosphine (tpdp) and bis-(diphenylphosphino)methane (dppm) were purchased from Aldrich and used as obtained. The complexes $(OC)_3$(N,N)Mo(L) [N,N = 1,10-phenanthroline, 4,7-dimethyl-1,10-phenanthroline; L = tpdp, dppm] were prepared according to Cano *et al.*[6] by reaction of $(OC)_4$Mo(N,N)[7] with the corresponding phosphine ligand. $(OC)_5$Mo(η^1-dppm) was prepared from $Mo(CO)_6$ and dppm as described by Hor.[8] Attempts to prepare the tpdp complex in this fashion failed. All reactions were carried out under an atmosphere of dry nitrogen in dried and degassed solvents.

In order to establish the *fac* or *mer* geometry of the complexes, ^{1}H NMR spectra in solution were obtained. Although both isomers belong to the same point group, C_s, they differ in the position of the mirror plane. These differences seem to have been overlooked in previous investigations. For comparison, spectra of the following ligands were also obtained.

1,10-Phenanthroline (in methanol-d_4): 8.77 H2, H9 [dd, 4.40 (H3, H8), 1.65 (H4, H7)]; 7.82 H4, H7 [dd, 8.06 (H3, H8), 1.65 (H2, H9)]; 7.31 H3, H8 [dd, 8.06 (H4, H7), 4.40 (H2, H9)]; 7.21 H5, H6 (s).

fac-$(OC)_3$(η^2-phen)Mo(tpdp) (in acetone-d_6): 9.51 H2, H9 [dd, 5.00 (H3, H8), 1.47 (H4, H7)]; 8.82 H4, H7 [dd, 8.24 (H3, H8), 1.47 (H2, H9)]; 8.25 H5, H6 (s); 8.04 H3, H8 [dd, 8.15 (H4, H7), 5.04 (H2, H9)].

fac-$(OC)_3$(η^2-phen)Mo(dppm) (in acetone-d_6): 9.20 H2, H9 [ddd, 5.04 (H3, H8), 1.3 (H4, H7), 1.3 (P)]; 8.40 H4, H7 [ddd, 8.15 (H3, H8), 1.32 (H2, H9), 1.3 (P)]; 7.99 H5, H6 (s); 7.49 H3, H8 [dd, 8.15 (H4, H7), 5.04 (H2, H9)]; 2.50 CH_2 [dd, 4.95 (P), 2.56 (P)].

4,7-Dimethyl-1,10-phenanthroline (in methanol-d_4): 8.55 H2, H9 [d, 4.40 (H3, H8)]; 7.16 H5, H6 (s); 7.07 H3, H8 [dd, 4.40 (H2, H9), 0.50 (Me)]; 2.26 Me [d, 0.50 (H3, H8)].

Table 1. Crystallographic Data for $(OC)_5$Mo(η^1-dppm)

empirical formula	$C_{30}H_{22}P_2MoO_5$
fw	620.39
cryst size (mm)	0.20 × 0.20 × 0.25
cryst syst	monoclinic
space group	*Pc*
a (Å)	8.866(5)
b (Å)	14.075(3)
c (Å)	11.293(2)
β (deg)	96.66(3)
V (Å^3)	1399.8(9)
Z	2
ρ_{calc} (g cm^{-3})	1.47
λ (Å)	Mo Kα, 0.710 69
μ (cm^{-1})	6.19
F(000)	628
θ range (deg)	25.0
no. of reflcns collcd	1741
no. of indepdt reflcns	1594
abs corr	ψ scans
no. of params	296
R (R_w)[a]	0.058 (0.164)
GOF[b]	1.08

[a] Residual index $R = \sum(|F_o| - |F_c|)/\sum|F_o|$; weighted residual $R_w = [\sum w(|F_o|^2 - |F_c|^2)^2/\sum w(F_o^2)^2]^{0.5}$. [b] Goodness-of-fit GOF = $S = [\sum w(F_o^2 - F_c^2)^2/(n - p)]^{0.5}$.

Unfortunately, analysis of the ^{1}H NMR spectra of the 4,7-dimethyl-1,10-phenanthroline molybdenum bisphosphine complexes was not possible due to the very low solubility of the compounds and overlap of the aromatic protons with the phenyl substituents at phosphorus.

X-ray Data Collection and Processing. A suitable crystal of $(OC)_5$Mo(η^1-dppm) was mounted in a glass capillary and placed on a Rigaku AFC5R diffractometer. Diffraction data were acquired at 23 °C. Crystal data and related details are given in Table 1. Intensity data were taken in the ω mode. Three check reflections, monitored every 150 reflections, showed a decrease of 0.8% during data collection; a linear correction factor was applied to the data. The data were corrected for Lorentz and polarization effects and for absorption using an empirical model (maximum and minimum transmission factors of 1.00 and 0.70). Scattering factors and corrections for anomalous dispersion were taken from a standard source.[9] Calculations were performed using the teXsan[10] and SHELXL-97[11] crystallographic software packages. The structure was solved by direct methods. Anisotropic thermal parameters were assigned to all non-hydrogen atoms. Hydrogen atoms were included but not refined. Final cycles of refinement converged to R = 0.058 and R_w = 0.164. The largest peaks in the final difference maps had values of 1.44 and −0.46 e Å^{-3}.

A single crystal of $(OC)_5$Mo(η^1-dppm), measuring approximately 1.5 × 1.8 × 0.4 mm, was grown by slow evaporation of a CH_2Cl_2/*n*-hexane (1:1) solution at room temperature and used for the single-crystal NMR experiment. The pale yellow crystal was glued to a hollow three-sided alumina cube measuring 4 mm on each side. The orientation of the crystal axis system was determined using an X-ray diffractometer. The crystal was oriented in such a way that the *a* axis, and approximately the *c* axis, are in the *X,Z* plane of the hollow cube (Figure 1). The orientation of the orthogonalized *a*bc* axis system in the NMR cube axis system *XYZ* is described by the Euler angles[12] α = 292.2°, β = 164.9°, γ = 116.7°.

NMR Experiments. NMR spectra of solutions were obtained using Bruker AC-250 (^{31}P, ^{1}H) and AMX-400 (^{1}H) spectrometers. Proton

(6) (a) Cano, M.; Campo, J. A.; Pérez-García, V.; Gutiérrez-Puebla, E.; Alvarez-Ibarra, C. *J. Organomet. Chem.* **1990**, *382*, 397. (b) Cano, M.; Campo, J. A.; Ovejero, P.; Heras, J. V. *J. Chem. Educ.* **1993**, *70*, 600.
(7) Hieber, W.; Mühlbauer, F. *Z. Anorg. Allg. Chem.* **1935**, *221*, 337.
(8) Hor, T. S. A. *J. Organomet. Chem.* **1987**, *319*, 213.
(9) *International Tables for X-Ray Crystallography*; D. Reidel Publishing Co.: Boston, MA, 1992; Vol. C.
(10) *teXsan for Windows*: *Crystal Structure Analysis Package*; Molecular Structure Corporation: The Woodlands, TX, 1997.
(11) Sheldrick, G. M.; Schneider, T. R. *SHELXL: High-Resolution Refinement*; Methods in Enzymology 277 (Macromolecular Crystallography, Part B); Carter, C. W., Sweet, R. M., Eds.; Academic Press: San Diego, 1997; pp 319−343.
(12) M. Mehring, *Principles of High Resolution NMR in Solids*, 2nd revised ed.; Springer-Verlag: Berlin, 1983.

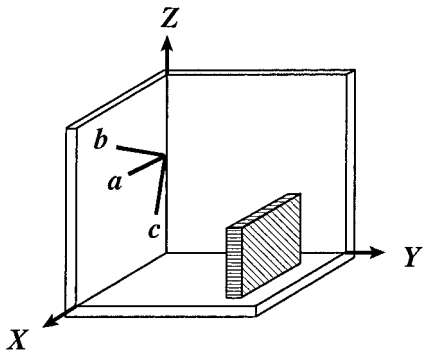

Figure 1. Relative orientations of the crystal holder, the NMR cube frame *X,Y,Z*, and the crystal axes *a,b,c* of the monoclinic crystal of $(OC)_5Mo(\eta^1$-dppm). The axes *a*, *b*, and *c* are approximately parallel to *X*, $-Y$, and $-Z$, respectively.

and ^{31}P chemical shifts were referenced with respect to internal TMS (^{1}H) and external 85% aq H_3PO_4 (^{31}P), respectively. Solid-state ^{31}P NMR experiments were carried out at 81.03 and 161.98 MHz using Bruker MSL-200 and AMX-400 spectrometers (B_0 = 4.7 and 9.4 T, respectively). The single-crystal ^{31}P NMR spectra were obtained on the MSL-200 using an automated single-crystal goniometer probe from Doty Scientific. The cube mount was placed into a hollow cubic receptacle in the goniometer of the probe, with the rotation axis perpendicular to the magnetic field. Rotations about the three orthogonal cube axes *X*, *Y*, and *Z* were performed in 9° intervals, controlled by an external stepper motor placed underneath the probe. The ^{31}P NMR spectra were acquired after cross-polarization (CP) using the Hartmann−Hahn match condition and under high-power proton decoupling, using ^{1}H pulse widths of 3.1 μs, contact times of 5 ms, and recycle delays of 1 min. Typically, 80 FID's were acquired, using a sweep width of 50 kHz and a time domain size of 1 K. Details concerning the analysis of single-crystal NMR experiments performed in our laboratory can be found elsewhere.[13−15]

Phosphorus-31 CP NMR spectra of stationary, MAS, or VAS powder samples were acquired using Bruker double-bearing MAS probes with 7 mm (4.7 T) or 4 mm (9.4 T) o.d. zirconia rotors, with 3.1−4.0 μs proton pulse widths and contact times of 3−5 ms. Chemical shifts were referenced with respect to external 85% aq H_3PO_4 by setting the peak of external $NH_4H_2PO_4$ to 0.8 ppm. Two-dimensional spin−echo measurements were carried out at 4.7 T. A standard spin−echo pulse sequence was used under CP and high-power ^{1}H decoupling conditions.[14,16] For each t_1 increment, 32−64 transients were collected. A total of 64 t_1 increments were acquired. After zero-filling once in each dimension, the data size for 2D FT was 512 × 128. Gaussian window-functions were applied to FIDs in both dimensions prior to 2D FT, and the final 2D spectrum was displayed in the magnitude mode. Zeeman magnetization-exchange experiments under conditions of rotational resonance were carried out by utilizing the DANTE sequence[17] to selectively invert the peak of the uncoordinated phosphorus, or by creating the difference magnetization directly using a four π-pulse sequence.[18]

Spectra of stationary powder samples and VAS spectra were calculated using WSolids; simulations related to the spin−echo experiments were carried out using SpinEcho. Both programs were developed in our laboratory and run on IBM compatible personal computers. Calculations of MAS spectra were performed using the programs NMRLAB[19] and CC2X[20] on an SGI Indy workstation.

Theoretical Background

For a homonuclear pair of spin-$^1/_2$ nuclei, the NMR Hamiltonian may be represented as the sum of Zeeman, chemical shielding, dipolar, and indirect spin−spin coupling interactions:[21]

$$H = H_Z + H_{CS} + H_D + H_J \tag{1}$$

In the case of a stationary sample, the frequencies and intensities of the four allowed transitions of an isolated spin pair are:[22]

$$\nu_1 = \frac{1}{2}(\Sigma + D + A) \qquad I_1 = 1 - \sin 2\zeta \tag{2}$$

$$\nu_2 = \frac{1}{2}(\Sigma + D - A) \qquad I_2 = 1 + \sin 2\zeta$$

$$\nu_3 = \frac{1}{2}(\Sigma - D + A) \qquad I_3 = 1 + \sin 2\zeta$$

$$\nu_4 = \frac{1}{2}(\Sigma - D - A) \qquad I_4 = 1 - \sin 2\zeta$$

$$\Sigma = \nu_A + \nu_B \tag{3}$$

$$\Delta = \nu_A - \nu_B \tag{4}$$

It is convenient to define Σ and Δ as the sum and difference of the resonance frequencies of spin A and spin B, considering only the Zeeman and chemical shielding interactions. The spin−spin coupling parameters *A* and *B* are dependent on the relative magnitudes of effective dipole−dipole and indirect spin−spin coupling. The mixing term *D* is dependent on the difference in resonance frequencies and strength of spin−spin interactions:

$$A = J_{iso} - R(3\cos^2\theta_R - 1) \tag{5}$$

$$B = J_{iso} + R(3\cos^2\theta_R - 1)/2 \tag{6}$$

$$D = \sqrt{\Delta^2 + B^2} \tag{7}$$

All interactions contributing to the spectrum are orientation dependent. In the case of chemical shielding, ν_A and ν_B are given by

$$\nu_i = \frac{\gamma B_0}{2\pi}[1 - (\sigma^i_{11}\sin^2\theta_i\cos^2\phi_i + \sigma^i_{22}\sin^2\theta_i\sin^2\phi_i + \sigma^i_{33}\cos^2\theta_i)] \tag{8}$$

where σ^i_{11}, σ^i_{22}, and σ^i_{33} are the principal components of the chemical shielding tensor at i = A and B, respectively, and the polar angles θ_i and ϕ_i describe the orientation of the applied magnetic field, $\mathbf{B}_0$, in the principal axis system (PAS) of the shielding tensor at *i*. The coupling parameters *A* and *B* are also

(13) (a) Power, W. P.; Mooibroek, S.; Wasylishen, R. E.; Cameron, T. S. *J. Phys. Chem.* **1994**, *98*, 1552. (b) Eichele, K.; Wasylishen, R. E. *J. Phys. Chem.* **1994**, *98*, 3108.
(14) Eichele, K.; Wu, G.; Wasylishen, R. E.; Britten, J. F. *J. Phys. Chem.* **1995**, *99*, 1030.
(15) Eichele, K.; Chan, J. C. C.; Wasylishen, R. E.; Britten, J. F. *J. Phys. Chem. A* **1997**, *101*, 5423.
(16) Rance, M.; Byrd, R. A. *J. Magn. Reson.* **1983**, *52*, 221.
(17) (a) Morris, G. A.; Freeman, R. *J. Magn. Reson.* **1978**, *29*, 433. (b) Nakai, T.; McDowell, C. A. *J. Magn. Reson., Ser. A* **1995**, *112*, 199.
(18) Geen, H.; Levitt, M. H.; Bodenhausen, G. *Chem. Phys. Lett.* **1992**, *200*, 350.
(19) Sun, B. Q.; Griffin, R. G. Unpublished.
(20) Levitt, M. H.; Raleigh, D. P.; Creuzet, F.; Griffin, R. G. *J. Chem. Phys.* **1990**, *92*, 6347.
(21) (a) VanderHart, D. L.; Gutowsky, H. S. *J. Chem. Phys.* **1968**, *49*, 261. (b) VanderHart, D. L.; Gutowsky, H. S.; *J. Chem. Phys.* **1969**, *50*, 1058. (c) Zilm, K. W.; Grant, D. W. *J. Am. Chem. Soc.* **1981**, *103*, 2913. (d) Power, W. P.; Wasylishen, R. E. *Annu. Rep. NMR Spectrosc.* **1991**, *23*, 1.
(22) van Willigen, H.; Griffin, R. G.; Haberkorn, R. A. *J. Chem. Phys.* **1977**, *67*, 5855.

orientation dependent; they depend on the angle, θ_R, between the external magnetic field and the internuclear vector.

The effective dipolar coupling, R, has contributions from the direct dipolar coupling constant, R_{DD}, and the anisotropy in the indirect spin−spin coupling, ΔJ:

$$R = R_{DD} - \Delta J/3 \tag{9}$$

$$R_{DD} = \frac{\mu_0}{4\pi}\frac{\hbar}{2\pi}\frac{\gamma^2}{\langle r^3\rangle} \tag{10}$$

$$\Delta J = J_{\parallel} - J_{\perp} \tag{11}$$

The dipolar coupling constant may also be influenced by vibrations and librations of the internuclear vector; thus, the value of r in eq 10 is a motionally averaged internuclear separation.[21c,23] In the above equations, it is assumed that $J_{\parallel}$ is parallel to the internuclear vector and that the **J** tensor is axially symmetric. Such an assumption could be justified in the case of directly bonded nuclei, as in the tpdp complexes, but seems dubious in the case of the complexes of dppm. The expressions above could be easily expanded to accommodate the general case. However, the experimental results (*vide infra*), and the single-crystal ^{31}P NMR experiment in particular, do not suggest the necessity of such generalizations. Note that the analysis of the single-crystal experiment does not depend on any assumptions regarding axial symmetry or coincidence of the PASs of the coupling interactions.

Finally, the intensities of the four transitions in eq 2 depend on the angle ζ,

$$\cos 2\zeta = \Delta/D$$
$$\sin 2\zeta = B/D \tag{12}$$

In summary, the NMR spectrum of a stationary powder sample containing an isolated spin pair is a superposition of four subspectra. As described in detail elsewhere,[14,21,22] analysis of such dipolar-chemical shift NMR spectra provides information about the orientation of chemical shift tensors relative to the internuclear vector (*vide infra*).

The line shapes in spectra of powder samples spinning off the magic angle at high spinning rates (i.e., no spinning sidebands) can be calculated using eq 2, if the scaling of the anisotropic interactions is taken into account by modifying eqs 5−8 as follows:[24]

$$\nu_i^S = \frac{\gamma B_0}{2\pi}\Big\{(1-\sigma^i_{iso}) - \frac{1}{2}(3\cos^2\vartheta - 1)[(\sigma^i_{11} - \sigma^i_{iso})\sin^2\theta_i^S\cos^2\phi_i^S + (\sigma^i_{22} - \sigma^i_{iso})\sin^2\theta_i^S\sin^2\phi_i^S + (\sigma^i_{33} - \sigma^i_{iso})\cos^2\theta_i^S]\Big\} \tag{13}$$

$$A^S = J_{iso} - R\,(3\cos^2\vartheta - 1)(3\cos^2\theta_R^S - 1)/2 \tag{14}$$

$$B^S = J_{iso} + R\,(3\cos^2\vartheta - 1)(3\cos^2\theta_R^S - 1)/4 \tag{15}$$

where ϑ is the angle between the external magnetic field and the spinning axis. Note that the polar angles θ_i^S, ϕ_i^S, and θ_R^S now describe the orientation of the spinning axis with respect to the PASs of the chemical shielding tensor and the internuclear vector, respectively.

Expressions for the free induction decays, $s(t_1)$ and $s(t_2)$, in the 2D spin−echo experiment[25] have been derived by Nakai and McDowell:[26]

$$s(t_1) = \cos^2 2\zeta[\exp(i\pi A t_1) + \exp(-i\pi A t_1)] + \frac{1}{2}\sin 2\zeta(1+\sin 2\zeta)[\exp(i\pi\{D-A\}t_1) + \exp(-i\pi\{D-A\}t_1)] - \frac{1}{2}\sin 2\zeta(1-\sin 2\zeta)[\exp(i\pi\{D+A\}t_1) + \exp(-i\pi\{D+A\}t_1)] \tag{16}$$

$$s(t_2) = (1-\sin 2\zeta)\exp\{i2\pi\nu_1 t_2\} + (1+\sin 2\zeta)\exp\{i2\pi\nu_2 t_2\} + (1+\sin 2\zeta)\exp\{i2\pi\nu_3 t_2\} + (1-\sin 2\zeta)\exp\{i2\pi\nu_4 t_2\} \tag{17}$$

The frequencies ν_i are given in eq 2. One can calculate the two-dimensional FID using $s(t_1,t_2) = s(t_1)s(t_2)$, or use eq 16 to calculate the F_1 projection directly. In order to test our calculations, we successfully simulated the 2D spin−echo ^{31}P NMR spectra of solid tetraethyldiphosphine disulfide. This is a relatively simple system which has been thoroughly investigated in our laboratory.[14] For an isolated homonuclear spin pair it is important to recognize that in general the calculated 2D spin−echo line shapes are very dependent on the chemical shift tensors (magnitudes and orientations) as well as the homonuclear spin−spin coupling interactions. For simplicity, only the F_1 projections are shown here. Generally, the experimental F_1 projections show a strong peak at 0 Hz because magnetization not refocussed by the echo sequence collects here. In the case of an A_2 spin system, a simple Pake doublet[27] results for the F_1 projection. Strong coupling effects may affect the F_1 projections for a more general homonuclear spin pair.[26,28]

For any given system, the relative orientations of the tensorial interactions are fixed and characteristic of the particular system under investigation. In order to take this property into account, it is convenient to express these orientations with respect to a common frame of reference. Ideally, this would be the molecular frame of reference. However, because we are dealing mainly with powder samples, the dipolar frame of reference is more suitable. As indicated in Figure 2, the Z axis of this reference frame is taken along the internuclear vector. Since the dipolar interaction is axially symmetric about this direction, the choice

(23) (a) Ishii, Y.; Terao, T.; Hayashi, S. *J. Chem. Phys.* **1997**, *107*, 2760. (b) Henry, E. R.; Szabo, A. *J. Chem. Phys.* **1985**, *82*, 4753.
(24) (a) Wu, G.; Wasylishen, R. E. *J. Chem. Phys.* **1994**, *100*, 4828. (b) Wu, G.; Wasylishen, R. E. *J. Chem. Phys.* **1994**, *100*, 5546. (c) Hoelger, C. G.; Aguilar-Parrilla, F.; Elguero, J.; Weintraub, O.; Vega, S.; Limbach, H. H. *J. Magn. Reson., Ser. A* **1996**, *120*, 46. (d) Challoner, R.; Harris, R. K.; Tossell, J. A. *J. Magn. Reson.* **1997**, *126*, 1.
(25) (a) Hahn, E. L. *Phys. Rev.* **1950**, *80*, 580. (b) Duijvestijn, M. J.; Manenschijn, A.; Smidt, J.; Wind, R. A. *J. Magn. Reson.* **1985**, *64*, 461. (c) Zilm, K. W.; Webb, G. G.; Cowley, A. H.; Pakulski, M.; Orendt, A. *J. Am. Chem. Soc.* **1988**, *110*, 2032. (d) Weliky, D. P.; Dabbagh, G.; Tycko, R. *J. Magn. Reson., Ser. A* **1993**, *104*, 10. (e) Engelsberg, M. In *Encyclopedia of Nuclear Magnetic Resonance*; Grant, D. M., Harris, R. K., Eds.; John Wiley & Sons: Chichester, U.K., 1996; Vol. 3, pp 1696-1700. (f) Engelsberg, M.; Yannoni, C. S. *J. Magn. Reson.* **1990**, *88*, 393.
(26) (a) Nakai, T.; McDowell, C. A. *J. Am. Chem. Soc.* **1994**, *116*, 6373. (b) Nakai, T.; McDowell, C. A. *Chem. Phys. Lett.* **1994**, *217*, 234.
(27) Pake, G. E. *J. Chem. Phys.* **1948**, *16*, 327.
(28) (a) Kumar, A. *J. Magn. Reson.* **1978**, *30*, 227. (b) Bodenhausen, G.; Freeman, R.; Morris, G. A.; Turner, D. L. *J. Magn. Reson.* **1978**, *31*, 75. (c) Kay, L. E.; McClung, R. E. D. *J. Magn. Reson.* **1988**, *77*, 258.

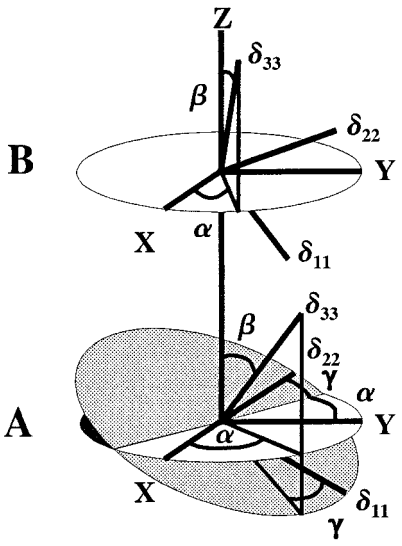

Figure 2. Dipolar frame of reference for a homonuclear spin pair, A and B. The *Z* axis of this frame is along the internuclear vector, r_{AB}, while *X* and *Y* are arbitrary. The orientations of the chemical shift tensors are expressed in terms of the Euler angles α,β,γ. The NMR spectrum of a homonuclear spin pair is invariant to any synchronous rotation of the chemical shift tensors about *Z*; only the difference of α values can be determined, at best.

of *X* and *Y* is arbitrary and the spectrum is invariant to any synchronous rotation of both chemical shift tensors about *Z*. Expressing the orientations of the chemical shift tensors in this frame by the Euler angles α, β, and γ, the actual values of α cannot be determined from an analysis of the spectra, only the difference in the values of α might affect the spectrum (*vide infra*). For this reason, the value of α for one of the phosphorus nuclei constituting the spin pair was set to zero arbitrarily.

Results and Discussion

Crystal Structure and Single-Crystal ^{31}P NMR of $(OC)_5Mo(\eta^1$-dppm), 3b. Single-crystal NMR measurements are capable of providing both the magnitude and orientation of chemical shift tensors. In the case of a monocoordinated diphosphine such as $(OC)_5Mo(\eta^1$-dppm), **3b**, one can simultaneously examine the phosphorus chemical shift tensors of both the "free" and metal-coordinated phosphorus nuclei. Such data will be crucial in improving our understanding of phosphorus chemical shifts and the origin of the coordination shift. Before undertaking a comprehensive single-crystal NMR study, it is desirable to know the crystal structure of the system of interest, particularly if one wishes to obtain the orientation of the shift tensors in the molecular frame of reference. Since the crystal structure of $(OC)_5Mo(\eta^1$-dppm) was unavailable, we carried out an X-ray diffraction study of this complex. The crystal is monoclinic, space group *Pc*, with two crystallographically equivalent molecules per unit cell. The two molecules are related by the mirror glide plane. Each molecule is relatively isolated from others with no unusual intermolecular contacts. Selected bond lengths and angles are listed in Table 2, and a perspective drawing of one molecule is shown in Figure 3. The P−P separation is 3.05 Å, which results in $R_{DD} = 693$ Hz (*cf.* eq 10).

Peak positions in the ^{31}P NMR spectra of a single crystal of **3b** as a function of crystal orientation in the magnetic field, so-called rotation patterns, are shown in Figure 4. Because the two molecules in the unit cell are magnetically nonequivalent, four doublets were generally observed for any given orientation

Table 2. Selected Bond Distances (Å) and Bond Angles (deg) for $(OC)_5Mo(\eta^1$-dppm)

Mo1−P1	2.536(7)	P2−C6	1.87(2)
Mo1−C1	2.09(3)	P2−C19	1.85(2)
Mo1−C2	1.99(2)	P2−C25	1.87(2)
Mo1−C3	1.98(3)	C1−O1	1.13(3)
Mo1−C4	2.07(3)	C2−O2	1.20(3)
Mo1−C5	2.08(3)	C3−O3	1.16(3)
P1−C6	1.85(2)	C4−O4	1.10(3)
P1−C7	1.85(2)	C5−O5	1.11(3)
P1−C13	1.83(3)		
P1−Mo1−C1	90.4(8)	C1−Mo1−C5	95(1)
P1−Mo1−C2	90.0(7)	C2−Mo1−C3	94(1)
P1−Mo1−C3	174.9(8)	C2−Mo1−C4	88(1)
P1−Mo1−C4	91.1(8)	C2−Mo1−C5	175(1)
P1−Mo1−C5	87.9(9)	C3−Mo1−C4	92(1)
C1−Mo1−C2	89(1)	C3−Mo1−C5	88(1)
C1−Mo1−C3	86(1)	C4−Mo1−C5	87(1)
C1−Mo1−C4	177(1)	Mo1−P1−C6	113.6(8)
Mo1−P1−C7	113.1(7)	Mo1−P1−C13	119.5(8)
C6−P1−C7	104(1)	C6−P1−C13	103(1)
C7−P1−C13	102(1)	C6−P2−C19	102(1)
C6−P2−C25	101(1)	C19−P2−C25	102(1)
P1−C6−P2	111(1)		

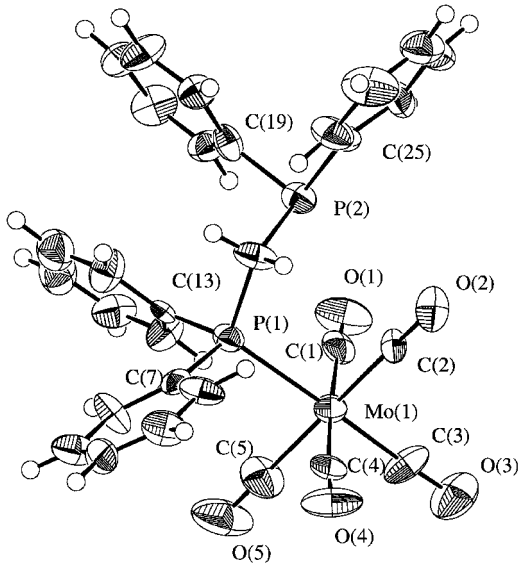

Figure 3. Perspective drawing of $(OC)_5Mo(\eta^1$-dppm) showing the atomic numbering scheme and 50% probability ellipsoids. Hydrogen atoms have an arbitrary radius of 0.1 Å.

of the single crystal in the applied magnetic field. Peak positions and splittings resulting from intramolecular spin−spin coupling were fit to an equation of the form:[13,14,29]

$$f_i(\varphi) = A_i + B_i \cos 2\varphi + C_i \sin 2\varphi \qquad (18)$$

using a linear least-squares procedure, where $f_i(\varphi)$ represents the orientation-dependent property, chemical shift (CS) or spin−spin coupling *C*, as a function of rotation progress, φ, about a given cube axis *i*. The resulting nine coefficients from the three rotations $i = X,Y,Z$, given in Table 3, were used to construct the chemical shift and spin−spin coupling tensors in the cube frame.[13,29] After diagonalization, the principal components of the CS and coupling tensors and their direction cosines in the cube frame were obtained.

The spin−spin coupling tensors *C* constructed from the coefficients in Table 3 contain contributions from both indirect

(29) Kennedy, M. A.; Ellis, P. D. *Concepts Magn. Reson.* **1989**, *1*, 109.

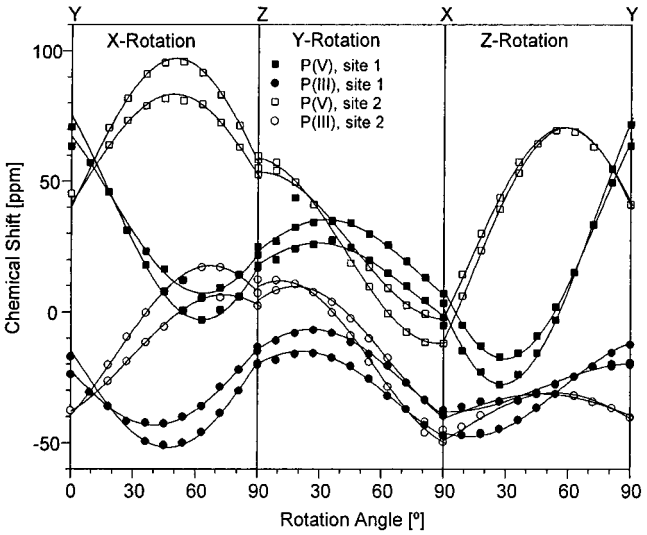

Figure 4. Peak positions in ^{31}P CP NMR spectra of a single crystal of $(OC)_5Mo(\eta^1$-dppm) as a function of crystal orientation in the magnetic field, for rotations about the cube *X*, *Y*, and *Z* axes, from left to right, respectively. Experimental data are represented by individual points, while linear least-squares fits to the data are shown as solid lines. The location of the crystallographic *b* axis is apparent at 10° of the *X* rotation.

Table 3. Linear Least-Squares Coefficients and Standard Deviations (in Parentheses) for the ^{31}P Chemical Shift δ (in ppm) and ^{31}P−^{31}P Spin−Spin Coupling Interaction *C* (in Hz) as a Function of Rotation of the Crystal of $(OC)_5Mo(\eta^1$-dppm) about the Cube *X*,*Y*,*Z* Axes

		A_i	B_i	C_i
δ(P1) site 1	*X*	45.5(4)	26.1(5)	−34.7(5)
	Y	11.6(2)	8.9(2)	16.9(2)
	Z	36.9(4)	−31.9(6)	−50.4(6)
δ(P1) site 2	*X*	47.9(4)	−7.2(5)	41.8(6)
	Y	24.5(2)	31.7(3)	−1.4(3)
	Z	17.4(4)	−24.2(6)	47.4(6)
δ(P2) site 1	*X*	−17.7(2)	−0.8(3)	−29.6(4)
	Y	−30.3(1)	13.1(2)	14.3(2)
	Z	−29.0(2)	−13.1(3)	−4.3(3)
δ(P2) site 2	*X*	−16.8(2)	−22.0(2)	18.5(2)
	Y	−19.0(2)	26.0(3)	14.1(3)
	Z	−42.5(4)	−2.5(5)	10.9(5)
C site 1	*X*	−119(28)	−513(38)	808(40)
	Y	540(14)	−111(19)	283(20)
	Z	−11(19)	623(26)	573(27)
C site 2	*X*	−151(18)	260(25)	−899(27)
	Y	158(12)	−591(17)	346(18)
	Z	400(13)	300(18)	−334(19)

spin−spin and direct dipole−dipole coupling; their traces are +136 Hz, in excellent agreement with $|J_{iso}|$ of 145 Hz observed in the ^{31}P CP/MAS spectrum of **3b**. This is the only example that we are aware of where the sign of ^2J(P,P) is known for the fragment M-PR_2-CH_2-PR_2. After subtracting J_{iso}, a coupling tensor axially symmetric within experimental error is obtained, characterized by an effective dipolar coupling constant, R = 691 Hz (see Table 4; standard deviation in the value of R is 43 Hz). The perfect agreement between R and R_{DD} = 693 Hz indicates that $\Delta^2J(^{31}P,^{31}P)$ is negligible (eq 9).

The crystal symmetry requires that the PASs of the magnetically distinct but crystallographically equivalent nuclei are related to each other via the twofold axis of the monoclinic crystal, corresponding to the crystal *b* axis. As an internal check on the agreement between single-crystal NMR and X-ray diffraction, the direction cosines of the *b* axis in the cube frame were calculated. From the PASs of the four CS and two spin−spin coupling tensors, one obtains −0.047(52), −0.974(8), 0.223(26), while the X-ray diffraction experiment yields: −0.055, −0.970, 0.237. The angle between these directions is 1.0°. The rotation patterns shown in Figure 4 reveal the location of *b* as the orientation where both magnetically distinct crystallographic sites become equivalent.

Table 4. Principal Components (in ppm) and Orientations of the Principal Axis Systems of the ^{31}P Chemical Shift and ^{31}P−^{31}P Spin−Spin Coupling Tensors Relative to the Orthogonalized Crystal Axis System *a***bc* of $(OC)_5Mo(\eta^1$-dppm) (Standard Deviations in Units of Least Significant Digits in Parentheses)

			*a**	*b*	*c*
P1	δ_{11}	102.6(13)	−0.3985(53)	0.8073(50)	0.4353(142)
	δ_{22}	30.1(5)	−0.4639(11)	0.2320(177)	−0.8550(42)
	δ_{33}	−40.9(3)	−0.7912(33)	−0.5426(1)	0.2820(90)
P2	δ_{11}	13.9(4)	−0.0653(98)	−0.4970(233)	−0.8653(126)
	δ_{22}	−31.8(3)	0.6847(105)	−0.6531(198)	0.3234(179)
	δ_{33}	−59.7(14)	−0.7260(90)	−0.5712(24)	0.3830(134)
R^a		691(43)	0.3389(9)	−0.7305(139)	−0.5928(176)

[a] Direction of unique component of the effective spin−spin coupling tensor.

After the CS and coupling tensors were transformed into the crystal axis system, the magnitudes and orientations of the principal components were averaged, as summarized in Table 4. Because of the existence of magnetically nonequivalent sites, there is a twofold ambiguity in assigning the orientation of the CS tensors to an orientation in the molecular frame of reference. However, under the assumption that the unique component of the spin−spin coupling tensor should be along the P−P vector, this ambiguity can be resolved.[30] For the assignment shown in Table 4, the angle between this unique component and the P−P vector is 0.7°, the same order of magnitude as the discrepancy in orientation of the C_2 axis.

Perspective drawings of the orientations of the chemical shift tensors in the molecular frame of reference are shown in Figure 5. The characteristic feature of the orientation for the coordinated phosphorus is that δ_{33} lies 11.2° off the Mo−P direction. Because δ_{11} and δ_{22} differ by 73 ppm in compound **3b**, one might expect that obvious reasons exist for their different magnitudes and orientations in the molecular frame, but we could find no distinct structural feature that might be responsible for the observed differences. The direction of δ_{11} is roughly perpendicular to the Mo1−P1−C13 plane, where C13 is an *ipso*-carbon. We note that this is the greatest Mo-P-C bond angle, 119.5°, compared to 113.1° and 113.6°. For the uncoordinated phosphorus of **3b**, the orientation of δ_{33} is in the general direction of the formal lone pair of electrons at phosphorus; however, the angles between δ_{33} and the directly bonded carbons are significantly different: 104° (C25), 118° (C6), and 125° (C19). Interestingly, electron density deformation maps from X-ray diffraction data from diphosphines indicate that the maximum electron density of the lone pair, lp, at phosphorus is not directed precisely along the apex of the PC_3 tetrahedron, but makes angles of 105°, 114°, and 130° with the P−C bonds.[31] The torsional angle between Mo1−P1 and lp−P2, viewed along the P1−P2 vector, is approximately 27° whereas the angle between the δ_{33} compounds for P1 and P2 is ca 7°.

^{31}P NMR Spectra of Powder Samples. The phosphorus chemical shift tensors and spin−spin coupling constants obtained

(30) (a) Lumsden, M. D.; Eichele, K.; Wasylishen, R. E.; Cameron, T. S.; Britten, J. F. *J. Am. Chem. Soc.* **1994**, *116*, 11129. (b) Lumsden, M. D.; Wasylishen, R. E.; Britten, J. F. *J. Phys. Chem.* **1995**, *99*, 16602. (c) Eichele, K.; Wasylishen, R. E.; Corrigan, J. F.; Taylor, N. J.; Carty, A. J. *J. Am. Chem. Soc.* **1995**, *117*, 6961.
(31) Bruckmann, J.; Krüger, C. *J. Organomet. Chem.* **1997**, *536/537*, 465.

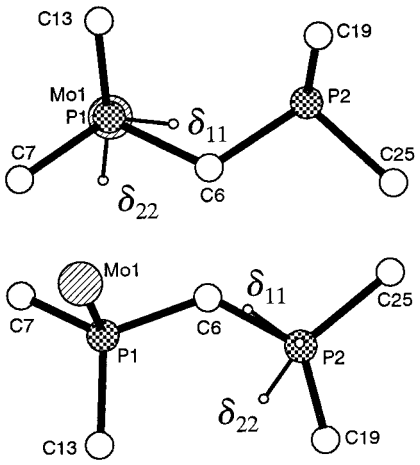

Figure 5. Orientation of the phosphorus chemical shift tensors in the molecular frame of reference for $(OC)_5Mo(\eta^1$-dppm), as determined by single-crystal ^{31}P NMR. The upper sketch shows the orientation for the phosphorus coordinated to molybdenum; the view is down the direction of the Mo−P bond. The lower sketch shows the orientation for the uncoordinated phosphorus, viewed down the direction of δ_{33}, which corresponds to the general direction of the formal lone pair of electrons.

from ^{31}P solid-state NMR spectra of the compounds investigated in the present study are summarized in Table 5. Also included are data reported by Nakai and McDowell[26] for the uncoordinated tpdp.

Uncoordinated dppm and tpdp. Powder samples of uncoordinated dppm have been studied by means of ^{31}P solid-state NMR by several groups. Bemi *et al.*[32] reported a single resonance at −23.6 ppm, using a magnetic field of 2.11 T. Roughly ten years later, Davies and co-workers[33] obtained spectra at 4.7 T. They reported an AB spectrum, with isotropic chemical shifts of −22.33 and −23.54 ppm, and $|^2J(P,P)| =$ 210 Hz. The observation of two different isotropic chemical shifts is in agreement with expectations based on the crystal structure, which contains two crystallographically nonequivalent phosphorus atoms in the molecule.[34] However, the coupling constant reported by Davies *et al.*[33] is significantly larger than the +125 Hz measured in solution by $^{13}C\{^1H,^{31}P\}$ triple resonance experiments.[35] Szalontai and co-workers[36] reinvestigated the ^{31}P MAS spectra of dppm at 6.34 T. They report a spinning rate dependence of the line shape for sample spinning rates between 4 and 5.5 kHz. Inappropriately using a procedure developed by Challoner *et al.*,[37] they reported an isotropic shift difference of 0.76 ppm and indicated that $^2J(P,P)$ could not be obtained using this procedure. The line shapes shown by Szalontai *et al.*[36] are indeed rather strange and cannot be reproduced at 4.7 T nor 9.4 T (*vide infra*).

Experimental CP/MAS ^{31}P NMR spectra of a powder sample of dppm obtained at 4.7 T with MAS frequencies of 3224 and 964 Hz are shown in Figure 6. The isotropic region ($\delta \approx -25$ ppm) of each spectrum consists of three peaks each separated by approximately 200 Hz. Notice that the relative intensities of the three peaks in the isotropic region are dependent on the spinning frequency. Also within each of the spinning sidebands, the three peaks have different relative intensities depending on the sideband order. The appearance of the three peaks in the spectra obtained at 4.7 T suggests the presence of a tightly coupled AB spin system. This was confirmed by obtaining a MAS ^{31}P NMR spectrum at 9.4 T (an expansion of the isotropic region is shown in the upper right inset of Figure 6). At the higher field, the four peaks of the AB spectrum are resolved and both the 4.7 and 9.4 T spectra can be simulated with $|^2J(P,P)| = 200$ Hz and $\Delta\delta = 1.6$ ppm. The calculated spectra at 4.7 and 9.4 T are the lower traces of the insets on the left and on the right of Figure 6, respectively. Our value of $|^2J(P,P)|$ in the solid state is in excellent agreement with the value reported by Davies *et al.*[33] Finally, it can be concluded that at a field strength of 2.11 T, as used by Bemi *et al.*,[32] the outer peaks of the AB multiplet were so weak that they disappeared within the wings of the strong inner peaks. The ^{31}P MAS spectra do indeed show a spinning rate dependence and a dependence of the line shape on the spinning sideband order, mostly in the relative intensities of the peaks, and to a smaller extent, a broadening at lower spinning rates (lower part of Figure 6). The ^{31}P chemical shift in solution, −21.6 to -23.0 ppm,[35,38] is similar to δ_{iso} observed in the solid state.

The ^{31}P NMR line shape of a stationary dppm sample (Figure 7) is characteristic of a chemical shift powder pattern; however some additional splittings can be discerned. These features arise from the fact that the two phosphorus nuclei are not equivalent and that they are coupled to one another via both the direct dipolar and indirect coupling interactions. The isotropic chemical shifts and the magnitude of J_{iso} were obtained from analysis of the MAS spectra at different fields. Estimates of the chemical shift anisotropies and their orientations were obtained from the static powder patterns at both 4.7 and 9.4 T (Figure 7). Using this information, the sign of J_{iso} and the magnitude of R were refined in the F_1 projection of the 2D spin−echo experiment (Figure 8a). The value of R obtained from the F_1 projection, 730 ± 30 Hz, agrees very well with the value calculated from the known P−P separation, 753 Hz. The sign of $^2J(P,P)$ is positive as found in solution. Keeping the spin−spin coupling interactions fixed, the chemical shift tensors including their orientations were refined, resulting in the values given in Table 5. The calculated spectra are sensitive to slight changes in the principal components or the orientations; however, it was possible to obtain good agreement between calculated and experimental spectra for more than one set of parameters. Fortunately, only the parameters given in Table 5 successfully accounted for the observed field dependence of the experimental spectra. It is therefore crucial to carry out such analyses using spectra obtained at different applied magnetic fields. One can appreciate this by considering three different theoretical single-crystal spectra shown at the bottom of Figure 7 (*vide infra*).

As indicated by the Euler angles given in Table 5, the PAS of the chemical shift tensors are not coincident. Therefore, the chemical shift difference between the phosphorus nuclei will be orientation dependent, as is the strength of the dipolar coupling. For the first simulated "single crystal spectrum", B_0 has polar angles of $\alpha = 86°$, $\beta = 110°$ with respect to the dipolar frame. In this case, the magnetic field is close to δ_{33} for P_B, but between δ_{22} and δ_{33} of P_A; it is also almost perpendicular to

(32) Bemi, L.; Clark, H. C.; Davies, J. A.; Fyfe, C. A.; Wasylishen, R. E. *J. Am. Chem. Soc.* **1982**, *104*, 438.
(33) Davies, J. A.; Dutremez, S.; Pinkerton, A. A. *Inorg. Chem.* **1991**, *30*, 2380.
(34) Schmidbauer, H.; Reber, G.; Schier, A.; Wagner, F. E.; Müller, G. *Inorg. Chim. Acta* **1988**, *147*, 143.
(35) Colquhoun, I. J.; McFarlane, W. *J. Chem. Soc., Dalton Trans.* **1982**, 1915.
(36) Szalontai, G.; Bakos, J.; Aime, S.; Gobetto, R. *Solid State Nucl. Magn. Reson.* **1993**, *2*, 245.
(37) (a) Challoner, R.; Nakai, T.; McDowell, C. A. *J. Chem. Phys.* **1991**, *94*, 7038. (b) Challoner, R.; Nakai, T.; McDowell, C. A. *J. Magn. Reson.* **1991**, *94*, 433. (c) Nakai, T.; Challoner, R.; McDowell, C. A. *Chem. Phys. Lett.* **1991**, *180*, 13.
(38) Horn, H. G.; Sommer, K. *Spectrochim. Acta Ser. A* **1971**, *27*, 1049.

Table 5. Phosphorus-31 Chemical Shift Tensors[a] and $^{31}P,^{31}P$ Spin−Spin Interactions[b] in Molybdenum Phosphine Complexes[c]

complex		δ_{iso}	δ_{11}	δ_{22}	δ_{33}	$J(^{31}P,^{31}P)$	$R(^{31}P,^{31}P)$	α[d]	β	γ
Ph_2P-PPh_2, tpdp[e]	**a**	−30.7 [f]	−17	−17	−57	−200	1665	0	78	0
								18	62	0
Ph_2P-CH_2PPh_2, dppm	**b**	−24.4 [g]	26	−28	−70	+200 [g]	730 [h]	0	85(3)	20(10)
		−26.0 [g]	19	−30	−67	+200 [g]	730 [h]	80(20)	82(5)	−36(10)
fac-$(OC)_3(\eta^2$-phen)-Mo(η^1-tpdp)	**1a**	24.3[i]	87	22	−36	−293[i]	1650	0	64(3)	10(10)
		−28.3[i]	6	−36	−55	−293[j]	1650	0(40)	77(2)	36(2)
fac-$(OC)_3(\eta^2$-phen)-Mo(η^1-dppm)	**1b**	39.5[j]	111	46	−39	*j, k*	625 [l]	0	55(5)	20(10)
		−27.6 [j]	30	−49	−63	*j, k*	625 [l]	40(40)	80(10)	10(10)
$(OC)_3(\eta^2$-9,10-Me_2-phen)Mo(η^1-tpdp)	**2a**	25.3[m]	96	27	−47	−320[m]	1675	0	75(3)	27(3)
		−11.4[m]	30	−19	−46	−320[m]	1675	118(10)	84(4)	54(4)
$(OC)_3(\eta^2$-9,10-Me_2-phen)Mo(η^1-dppm)	**2b**	21.9[n]	82	38	−55	+107[n]	650	0	80(10)	30(5)
		−32.8[n]	15	−48	−65	+107[n]	650	0(40)	80(15)	15(15)
$(OC)_5Mo(\eta^1$-dppm)	**3b**	31.3[o]	101	34	−41	+145[o]	690 [p]	0	87(3)	11(3)
		−25.2[o]	16	−32	−60	+145[o]	690 [p]	7(3)	86(3)	30(3)
mer-$(OC)_3(\eta^2$-phen)-Mo(η^1-dppm)	**1b′**	15.9[q]	74	1	−27	*k, q*				
		−20.6[q]	31	−41	−51	*k, q*				

[a] In ppm relative to external 85% aq H_3PO_4, with high-frequency shifts positive; errors in the principal components are estimated to be 2 ppm, except for **1b′** (5 ppm). [b] In Hz; errors in J_{iso} are 5 Hz, and errors in R are 30 Hz. [c] phen = 1,10-phenanthroline; Me_2phen = 4,7-dimethyl-1,10-phenanthroline; tpdp = tetraphenyldiphosphine; dppm = bis(diphenylphosphino)methane. [d] The value of α of the first phosphorus was set to zero arbitrarily (see text). [e] Values taken from ref 26a. [f] Chemical shift in solution: −14.1 ppm (ref 40). [g] Chemical shift in solution: −21.6 to −23.0 ppm (refs 35 and 38); $^2J(^{31}P,^{31}P)$ = +125 Hz (ref 35). [h] Calculated from P−P separation of 2.97 Å: 753 Hz. [i] Chemical shifts (and coupling constants) in CH_2Cl_2 solution: 27.2 ppm (d, 312 Hz) and −17.4 ppm (d, 312 Hz). [j] Chemical shifts (and coupling constants) in solution: 28.7−29.3 ppm (d, 63.5−70 Hz) and −27.0 to −27.6 ppm (d, 63.5−70 Hz) (refs 6, 43c, and 45). [k] Less than 20 Hz in the solid state. [l] Calculated from P−P separation of 3.16 Å (ref 6): 625 Hz. [m] Chemical shifts (and coupling constants) in CH_2Cl_2 solution: 26.6 ppm (d, 313 Hz) and −17.1 ppm (d, 313 Hz). [n] Chemical shifts (and coupling constants) in CH_2Cl_2 solution: 27.4 ppm (d, 73 Hz) and −27.8 ppm (d, 73 Hz). [o] Chemical shifts (and coupling constants) in solution: 28.1−28.3 ppm (d, 112−114 Hz) and −24.9 to −25.0 ppm (d, 112−114 Hz) (refs 43c, 44c, and 45). [p] Calculated from P−P separation of 3.053 Å: 693 Hz. [q] Chemical shifts (and coupling constants) in solution: 20.3 ppm (d, 61.8 Hz) and −27.7 ppm (d, 61.8 Hz) (ref 6).

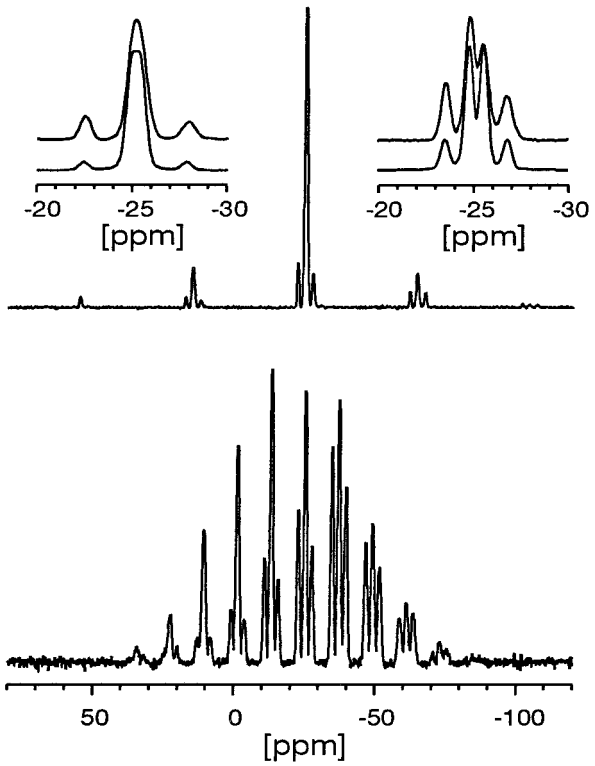

Figure 6. Phosphorus-31 CP/MAS NMR spectra of powder samples of dppm obtained at 4.7 T with spinning rates of 3224 Hz (upper) and 964 Hz (bottom). The insets show the isotropic regions of MAS spectra obtained at 4.7 T (left) and 9.4 T (right), together with simulations using a high-resolution Hamiltonian. The upper spectrum of each inset is the experimental spectrum.

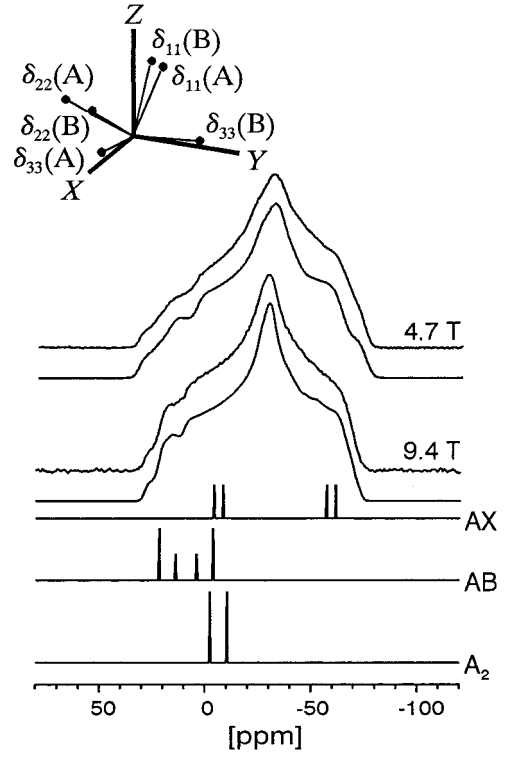

Figure 7. Phosphorus-31 CP NMR experimental (upper) and calculated (lower) spectra of stationary powder samples of dppm obtained at 4.7 and 9.4 T. The lower traces are theoretical spectra for three different orientations of a single crystal in the applied magnetic field of 9.4 T (see text). Relative orientations of the chemical shift tensors in the dipolar frame of reference are indicated in the upper left corner.

the P−P vector. Because J_{iso} has the same sign as R, their combined effect is a reduction of the splitting. In summary, the chemical shift difference is much larger than the spin−spin coupling, and at this particular orientation the spin pair behaves like an AX spin system. For $\alpha = 106°$, $\beta = 31°$, the magnetic field is close to δ_{11} of both ^{31}P nuclei; the chemical shift difference is small and the coupling is relatively strong, resulting in an AB spin system (due to the presence of the dipolar coupling, the weaker peaks may switch to the inside of the multiplet, contrary to the case in solution). Finally, if the applied

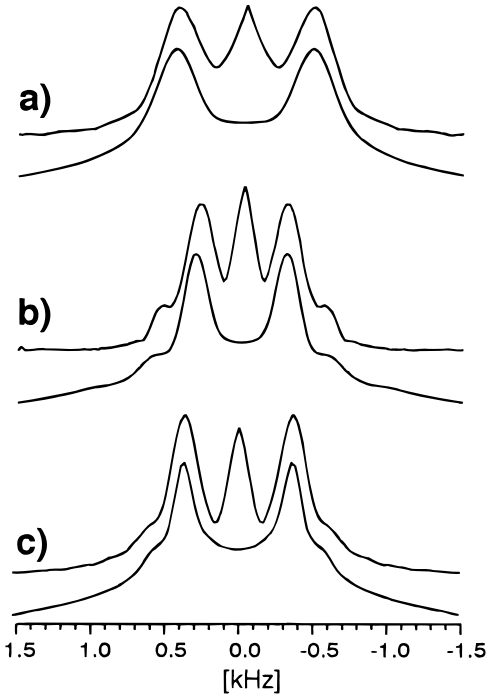

Figure 8. F_1 projections from two-dimensional ^{31}P spin−echo spectra of stationary powder samples of (a) dppm, (b) *fac*-(OC)$_3$(η^2-phen)Mo(η^1-dppm), and (c) *fac*-(OC)$_3$(η^2-Me$_2$phen)Mo(η^1-dppm), obtained at 4.7 T. Spectra were calculated using the parameters given in Table 5. The different appearance of the spectra for these compounds arises mainly from the different relative magnitudes of the dipolar coupling constant and the isotropic spin−spin coupling constant. The artifact at zero in the experimental spectra is discussed in the text.

magnetic field is along the *Z* axis, the spin−spin interactions are at a maximum and the chemical shift difference is close to zero, resulting in an A_2 spectrum. It is this mixture of different spin systems which makes the dipolar-chemical shift NMR spectra of homonuclear spin pairs sensitive to the relative orientations of the chemical shift tensors. An indication of this admixture of spin systems can also be recognized in ^{31}P NMR spectra obtained with slow MAS (bottom trace of Figure 6). The low-frequency portion of the MAS spectrum arises predominantly from crystallites constituting AX spin systems; therefore, the outer peaks of the spinning sidebands are relatively intense. On the other hand, the high frequency part of the spectrum is dominated by contributions from AB and A_2 spin systems, resulting in relatively weak outer peaks in this region.

As pointed out in the theoretical section, for homonuclear spin pairs such as the phosphorus spin pair of dppm, one can only determine the relative orientation of the chemical shift tensors in the dipolar frame of reference. We can only speculate about the orientation in the molecular frame. Usually, it is assumed that the most shielded direction in phosphine derivatives is along the putative direction of the lone pair of electrons, as confirmed by the single-crystal NMR experiment on **3b**. Because the exact locations of the lone pairs in dppm are not known, we estimate from the crystal structure[34] that they might make angles of 80−85° with respect to the P−P axis, and have a torsional angle of 60−70° about this axis. The experimental Euler angles $\beta = 82°$, and the difference in α of 80° are consistent with δ_{33} lying along or close to the orientation of the formal lone pair on phosphorus.

As already mentioned, the value of ^2J(P,P) in the solid state is +200 Hz, significantly greater than the conformationally averaged value measured in solution, +125 Hz. Values of ^2J(P,P) are known to be very dependent on the orientation of the phosphorus lone pairs. For example, in the X_2PNRPX_2 fragment, ^2J(P,P) can assume values ranging from −35 Hz to values in excess of +700 Hz.[39] The value of ^2J(P,P) measured here for dppm is important because the conformation of the molecule is known from X-ray diffraction studies.[34]

Uncoordinated tpdp has been investigated recently by Nakai and McDowell[26] using two-dimensional spin−echo experiments on stationary powder samples. They reported that the two phosphorus nuclei of the molecule have axially symmetric chemical shift tensors with identical principal components but different orientations in the dipolar frame of reference. In solution, the chemical shift has been reported as −14.1 ppm.[40]

Metal Phosphine Complexes. The ^{31}P CP/MAS spectra of the metal phosphine complexes studied here typically show two doublets. The doublet at lowest frequency, between −11 and −33 ppm, was assigned to the uncoordinated phosphorus of the bisphosphine ligand, while the doublet at higher frequency, between 16 and 40 ppm, was assigned to the phosphorus coordinated to molybdenum. Support for this assignment comes from the presence of ^{95,97}Mo satellites flanking the high-frequency doublets. Although these satellites could not be analyzed because most of the multiplet is covered by the central doublet of uncoupled phosphorus, the overall width is consistent with the ^1J(^{95,97}Mo,^{31}P) values observed for other typical complexes of molybdenum.[41] The signs and magnitudes of ^1J(^{31}P,^{31}P) determined here for the complexes of tpdp are negative. For uncoordinated diphosphines, solution NMR studies also indicate negative signs for ^1J(^{31}P,^{31}P).[40] Similarly, the signs of ^2J(^{31}P,^{31}P) have been determined for a variety of dppm derivatives and similar compounds.[42] The latter couplings have been found to be positive, except for diselenides where small negative values have been reported.[35] Given the drastic variations in the magnitude of ^2J(^{31}P,^{31}P) observed for the dppm complexes here (Table 5), ranging from +200 Hz in dppm itself to near zero in *fac*-(OC)$_3$(η^2-phen)Mo(η^1-dppm), it seems possible that in some environments the sign of this coupling may be negative. The values of ^2J(^{31}P,^{31}P) observed for (OC)$_3$(η^2-N,N)M(η^1-dppm) (M = Cr, Mo, W; N,N = phen, bpy) complexes in solution,[43] 51−70 Hz, and for (OC)$_n$M(η^1-dppm) (M = Mo, W, n = 5; M = Fe, n = 4), 80-114 Hz,[8,43c,44] clearly indicate some sensitivity of this coupling to structural features. As with other two-bond indirect spin−spin coupling constants involving phosphorus(III), the orientation of the formal electron lone pair on P(III) is undoubtedly important. For example, the value of ^2J(^{31}P,^{31}P) for **1b** in solution, 63.6−70 Hz,[6,43c,45] is much larger than the value in the solid state, which is less than

(39) Keat, R.; Manojlović-Muir, L.; Muir, K. W.; Rycroft, D. S. *J. Chem. Soc., Dalton Trans.* **1981**, 2192.
(40) Aime, S.; Harris, R. K.; McVicker, E. M.; Fild, M. *J. Chem. Soc., Dalton Trans.* **1976**, 2144.
(41) (a) Lindner, E.; Fawzi, R.; Mayer, H. A.; Eichele, K.; Pohmer, K. *Inorg. Chem.* **1991**, *30*, 1102. (b) Eichele, K.; Wasylishen, R. E.; Kessler, J. M.; Solujić, L.; Nelson, J. H. *Inorg. Chem.* **1996**, *35*, 3904. (c) Eichele, K.; Wasylishen, R. E.; Maitra, K.; Nelson, J. H.; Britten, J. F. *Inorg. Chem.* **1997**, *36*, 3539.
(42) (a) Colquhoun, I. J.; McFarlane, W. *J. Chem. Res., Synop.* **1978**, 368. (b) Harris, R. K.; Woplin, J. R.; Issleib, K.; Lindner, R. *J. Magn. Reson.* **1972**, *7*, 291. (c) Carty, A. J.; Harris, R. K. *J. Chem. Soc., Chem. Commun.* **1967**, 234.
(43) (a) Hor, T. S. A. *Inorg. Chim. Acta* **1987**, *128*, L3. (b) Cano, M.; Campo, J. A.; Ovejero, P.; Heras, J. V. *J. Organomet. Chem.* **1990**, *396*, 49. (c) Rottink, M. E.; Angelici, R. J. *Inorg. Chem.* **1993**, *32*, 2421.
(44) (a) Chan, H. S. O.; Hor, T. S. A.; Chiam, C. S. M.; Chong, T. C. *J. Therm. Anal.* **1987**, *32*, 1115. (b) Benson, J. W.; Keiter, E. A.; Keiter, R. L. *J. Organomet. Chem.* **1995**, *495*, 77. (c) Jacobsen, G. B.; Shaw, B. L.; Thornton-Pett, M. *J. Chem. Soc., Dalton Trans.* **1987**, 1509.
(45) Hor, T. S. A. *Inorg. Chim. Acta* **1987**, *128*, L3.

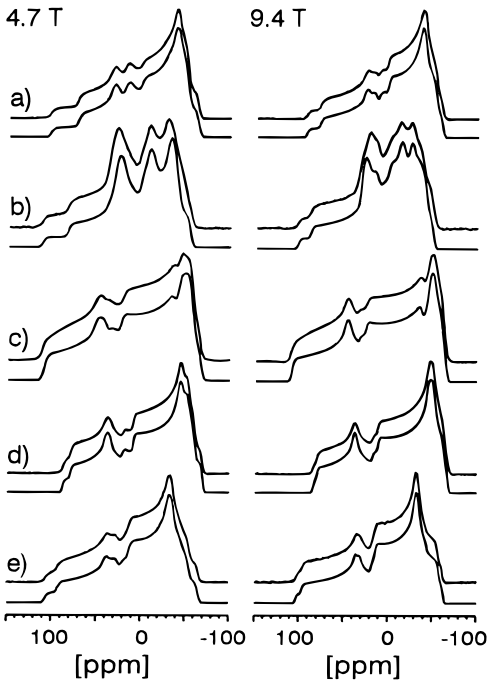

Figure 9. Phosphorus-31 NMR spectra of stationary powder samples of the bisphosphine complexes studied, obtained at applied fields of 4.7 T (left column) and 9.4 T (right column), together with theoretical spectra calculated using the parameters given in Table 5. The compounds are (a) *fac*-$(OC)_3(\eta^2$-phen)Mo(tpdp), (b) *fac*-$(OC)_3(\eta^2$-Me_2phen)Mo(tpdp), (c) *fac*-$(OC)_3(\eta^2$-phen)Mo(dppm), (d) *fac*-$(OC)_3$-$(\eta^2$-Me_2phen)Mo(dppm), (e) $(OC)_5$Mo(dppm).

20 Hz (based on typical line widths observed for the other complexes). This difference is almost certainly associated with the different conformations of the $MoP(Ph)_2CH_2P(Ph)_2$ fragment adopted in solution and the solid state. Further confirmation comes from the fact that δ_{iso} of P(V) in **1b** is shifted 10 ppm to higher frequencies from the shift observed in solution, an amount which is beyond the typical differences between solid and solution state.

Phosphorus-31 NMR spectra of stationary powder samples of the complexes studied here are collected in Figure 9. From these spectra, it is clear that the chemical shift anisotropies of the coordinated and uncoordinated phosphorus overlap widely; generally, the metal-coordinated phosphorus has a greater chemical shift anisotropy (i.e., larger span) than the uncoordinated phosphorus. This overlap makes it desirable to obtain the different parameters from different experiments. Isotropic chemical shifts and coupling constants were determined from the MAS spectra. Effective dipolar couplings and the sign of J_{iso} were determined from the F_1 projections of 2D spin−echo experiments. A comparison of the F_1 projections of dppm (Figure 8) and tpdp complexes (Figure 10) reveals two distinct differences. First, due to the much smaller P−P separation in the tpdp complexes, the spin−spin couplings are much stronger. Secondly, for the dppm compounds, the horns of the patterns are much closer to the shoulders than in a pure Pake doublet, up to hiding them in dppm itself. This indicates that J_{iso} and R have the same sign (*i.e.*, almost certainly positive). However, for the tpdp complexes, J_{iso} and R have different signs (*i.e.* J_{iso} is probably negative).[46] In most cases, the F_1 projections can be interpreted as arising from AX spin systems, except for the case of **2a**, which exhibits some second-order character.

(46) Eichele, K.; Wasylishen, R. E.; Schurko, R. W.; Burford, N.; Whitla, W. A. *Can. J. Chem.* **1996**, *74*, 2372.

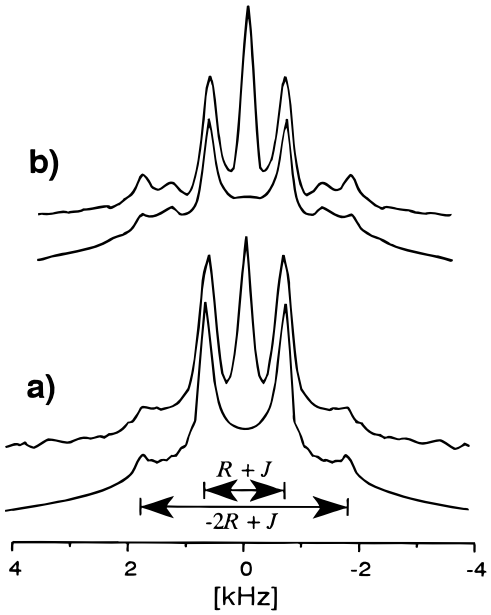

Figure 10. F_1 projections from two-dimensional ^{31}P spin−echo spectra of powder samples of (a) *fac*-$(OC)_3(\eta^2$-phen)Mo(η^1-tpdp), and (b) *fac*-$(OC)_3(\eta^2$-Me_2phen)Mo(η^1-tpdp), obtained at 4.7 T. Spectra were calculated using the parameters given in Table 5. In (b), residual chemical shift effects cause additional peaks to appear, while (a) can be interpreted on the basis of the AX approximation.

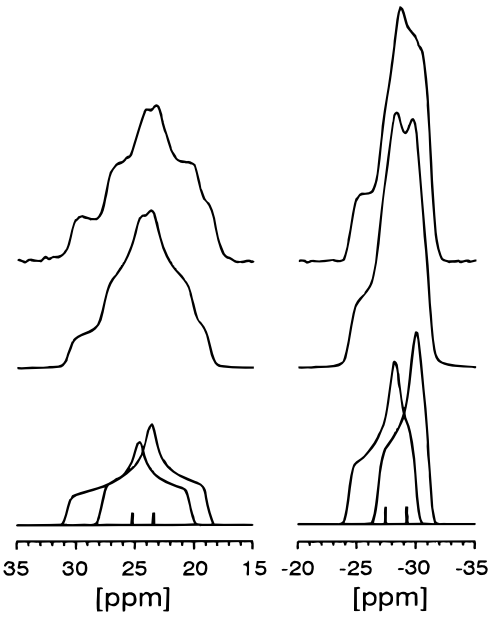

Figure 11. Isotropic regions in experimental and theoretical ^{31}P spectra of a powder sample of *fac*-$(OC)_3(\eta^2$-phen)Mo(η^1-tpdp) spinning at an angle of 51.6° with respect to the external magnetic field of 9.4 T. The theoretical spectrum was calculated for the fast spinning limit. The bottom trace displays the decomposition into the scaled subspectra, the two lines separated by $^1J(^{31}P,^{31}P)$ indicate the doublets of the corresponding MAS spectrum. Compare to the static spectrum in Figure 9a, right column.

Separate scaled powder patterns for the two nonequivalent phosphorus nuclei can be observed by spinning the sample about an axis different than the magic axis (VAS); see Figure 11. Unfortunately, the hardware available required spinning the sample at angles close to the magic angle, resulting in significant scaling factors. Thus, the principal components of the chemical shift tensors determined in this manner have relatively large uncertainties. Refinement of the principal components was

carried out by simulating the static powder patterns obtained at two applied magnetic fields, Figure 9. The parameters obtained from the combined analysis are collected in Table 5. The values of the effective dipolar coupling constants obtained for the dppm complexes are in good agreement with the values calculated from the P−P separation, where known.

Unfortunately, none of the crystal structures of the tpdp complexes are known, and we were unable to obtain single crystals of suitable quality for X-ray diffraction. On the basis of P−P distances found in compounds containing P−P bonds,[47] 2.15−2.245 Å, the calculated value of R_{DD} is 1984−1743 Hz. From the data in Table 5, it appears that the effective couplings obtained from NMR spectra are consistently too small by approximately 200 Hz. This could be attributed to a contribution from anisotropy in the indirect spin−spin coupling constant.[14,48,49] However, given that a reduction of R_{DD} on the same order of magnitude was observed for tetraethyldiphosphine disulfide, with a very small value of $^1J(^{31}P,^{31}P)$, it could also be argued that librational averaging omnipresent in crystals could be responsible. Considering the current uncertainties in the actual P−P bond lengths, it is futile to speculate further.

Phosphorus Chemical Shift Tensors. We found in the single-crystal study of **3b** that the direction of greatest shielding lies close (11°) to the direction of the Mo-P bond. Previously, we found for another pentacarbonyl molybdenum complex that one principal component lies near the Mo−P bond (8°), although in that particular case this was δ_{22} with a chemical shift of −40 ppm.[41c] For the molybdenum phosphine complexes studied to date,[41] phosphorus chemical shift values in the range of −25 to −55 ppm seem to be characteristic for the direction of the Mo−P bond, in most cases corresponding to δ_{33}. While this observation may naively be interpreted as confirmation that the direction of highest shielding corresponds to the direction of highest electron density (due to the metal), this view is certainly not justified. If this interpretation were correct, one should expect this direction to show the greatest change in chemical shift when the free ligand coordinates to the metal. However, it is the directions perpendicular to the metal- or lone pair-phosphorus direction that generally change most dramatically. It is primarily the mixing of the orbitals associated with the P−C bonds that contributes to the chemical shift in the direction of the metal or lone pair, and the chemical shift change along this direction reflects the effect of the metal on the substituent orbitals upon coordination. The situation perpendicular to the Mo−P direction is more complicated, as contributions from the P−C and Mo−P bonds may play a role. In many cases, a clear deviation of the chemical shift tensor from axial symmetry was observed, although the two single-crystal ^{31}P NMR studies available so far do not shed light on the cause of this observation. It seems that δ_{11} is directed perpendicular to the plane containing the greatest Mo−P−C angles. Hopefully, the emerging *ab initio* calculations of chemical shifts can further our understanding here.

As indicated above, the orientation of δ_{33} seems to correspond to the general direction of the Mo−P or lp−P vector. Hence, it is not too surprising that the β angles for the two tpdp complexes are rather similar. However, the difference in α indicates that the relative orientations of Mo−P and lp−P should be different. For **1a**, they indicate a syn or anti conformation, while for **2a** a gauche conformation would be predicted (note the differences in δ_{iso} of the uncoordinated phosphorus). The situation is more complicated in the case of the dppm complexes.

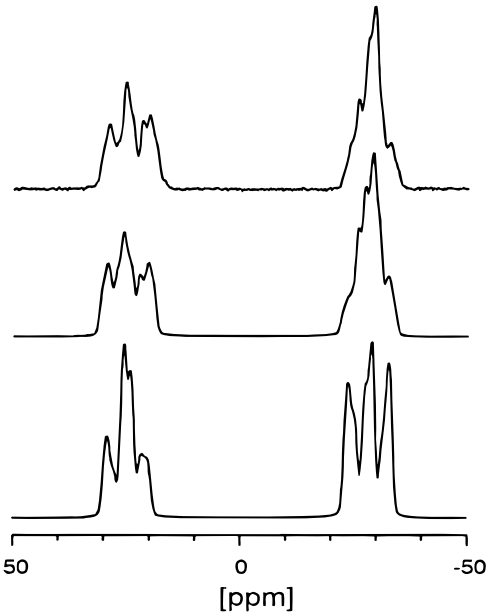

Figure 12. Experimental and calculated 4.7 T ^{31}P MAS spectra of a powder sample of *fac*-$(OC)_3(\eta^2$-phen)Mo(η^1-tpdp) spinning at 4.3 kHz under the condition of rotational resonance ($n = 1$). The experimental spectrum is the upper trace. The spectra were calculated using the parameters given in Table 5, except for the spectrum of the bottom trace, for which the sign of $^1J(^{31}P,^{31}P)$ was set positive.

Rotational-Resonance Experiments. These experiments have been developed to recover homonuclear dipolar coupling constants from high-resolution NMR experiments conducted with MAS. Most applications have involved biological macromolecules containing isolated spin pairs. Here we wish to explore the utility of this experiment in measuring $R(^{31}P,^{31}P)$ in bisphosphine molybdenum complexes. While the ^{31}P MAS spectra of the metal complexes generally exhibit two doublets (except for **1b**, where $J(^{31}P,^{31}P)$ is small), the line shape changes if the spinning speed is adjusted such that an integer multiple of the spinning speed matches the chemical shift difference between the two phosphorus nuclei, $n\nu_r = \nu_L[\delta_{iso}(A) - \delta_{iso}(B)]$, with $n = 1, 2, 3, ...$ This is the so-called rotational-resonance condition of order n.[50]

Rotational resonance line shapes for *fac*-$(OC)_3(\eta^2$-phen)Mo-(η^1-tpdp), **1a**, are shown in Figure 12 ($n = 1$). The calculated spectrum (center trace of Figure 12) depends on the magnitude and orientation of the internuclear vector relative to the principal components and orientation of the phosphorus shift tensors. In addition, the lower trace in Figure 12 indicates that the line shapes depend on the sign of the indirect spin−spin coupling constant, $^1J(P,P)$.

The flip-flop operator of the dipolar Hamiltonian is largely responsible for the dramatic line shape variations that result under conditions of rotational resonance. When the rotational-resonance condition is not met, this term of the Hamiltonian is largely quenched. The efficiency of this flip-flop term depends

(47) (a) Richter, R.; Kaiser, J.; Sieler, J.; Hartung, H.; Peter, C. *Acta Crystallogr.* **1977**, *B33*, 1887. (b) Kaiser, J.; Hartung, H.; Lengies, E.; Richter, R.; Sieler, J. *Z. Anorg. Allg. Chem.* **1976**, *422*, 149. (c) Carriedo, G. A.; Fernández, L.; Goméz, P.; García-Granda, S.; Velázquez, A. M. *Acta Crystallogr.* **1995**, *C51*, 20. (d) Turnbull, M. M.; Wong, E. H.; Gabe, E. J.; Lee, F. L. *Inorg. Chem.* **1986**, *25*, 3189. (e) Wong, E. H.; Ravenelle, R. M.; Gabe, E. J.; Lee, F. L.; Prasad, L. *J. Organomet. Chem.* **1982**, *233*, 321.
(48) (a) Tutunjian, P. N.; Waugh, J. S. *J. Chem. Phys.* **1982**, *76*, 1223. (b) Tutunjian, P. N.; Waugh, J. S. *J. Magn. Reson.* **1982**, *49*, 155.
(49) Grimmer, A.-R.; Peter, R.; Fechner, E. *Z. Chem.* **1978**, *18*, 109.
(50) Andrew, E. R.; Bradbury, A.; Eades, R. G.; Wynn, V. T. *Chem. Phys. Lett.* **1963**, *4*, 99.

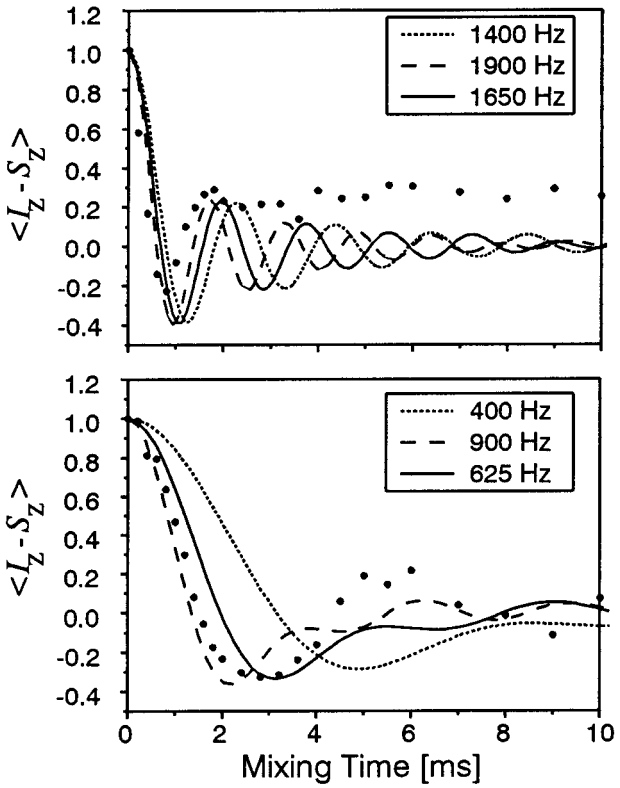

Figure 13. Difference magnetization as a function of mixing time in Zeeman-exchange experiments under rotational resonance for powder samples of *fac*-$(OC)_3(\eta^2$-phen)Mo(η^1-tpdp), top, and *fac*-$(OC)_3(\eta^2$-phen)Mo(η^1-dppm), bottom. Selective inversion has been achieved using a DANTE sequence consisting of 5−6 pulses. Experimental data are shown as solid circles.

on the magnitude of the direct dipolar coupling constant, and therefore experiments have been devised to measure the strength of this interaction, and hence internuclear distances, under rotational resonance.[51] Basically, these experiments consist of a selective inversion of one of the peaks, followed by a mixing time to allow for magnetization exchange between the two spins and a measurement of the transverse magnetization. Recently, it has been shown that a four π-pulse sequence can be used to create the difference magnetization directly.[18] Plots of the difference magnetization versus the mixing time show damped oscillations, which can be compared with theoretical curves calculated numerically (Figure 13). Although the experimental data shown in Figure 13 show oscillations and decays of the correct order of magnitude, some systematic discrepancies are also evident. For both systems, the decay is faster than anticipated under the assumption of isolated spin pairs. The systems most widely studied using this technique have been ^{13}C spin pairs in biologically relevant systems. Usually, the specifically labelled compound has been immersed in a matrix of the natural abundance compound to minimize intermolecular contributions. In the case of phosphorus, this is not possible, although our intention in using the phenanthroline ligand was to introduce sterically demanding ligands in order to increase intermolecular distances. We encountered several problems applying rotational-resonance experiments to the organometallic compounds investigated here. Similar to TOSS experiments, the four π-pulse sequence relies on the balanced effects of π pulses and free evolution, synchronized with the sample spinning.[18] With high spinning rates, the delays become short relative to the pulses, and the method is less efficient.[52] The broad multiplets pose another problem as they also dephase during the free evolution (there is no on-resonance position). Hence, the DANTE sequence is more efficient for the systems under study. However, the selective inversion of the magnetization of one spin in two-spin systems is problematic when the two spins are strongly indirectly spin−spin coupled (i.e., J is large) as one needs to invert a relatively wide area without perturbing the other spin. Nevertheless, rotational-resonance experiments have some potential in obtaining approximate values of R when no other method is available. We found through many numerical simulations that the short time behavior of the magnetization-exchange experiments (for $n = 1, 2$) is not sensitive to the relative orientations of the phosphorus chemical shift tensors. Previous workers have also made this observation in their investigation of other systems.[51e]

Conclusions

We have utilized several NMR techniques to characterize homonuclear spin pairs in the solid state. The number of parameters required to fully characterize the spectra is relatively large: three principal components for each chemical shift tensor and the accompanying three Euler angles required to relate their orientation to the dipolar frame of reference, as well as the spin−spin and dipole−dipole coupling constants. The single-crystal NMR experiment is the most powerful experiment in this respect as it allows the separate analysis of chemical shift and spin−spin coupling interactions and yields the tensor orientations in the molecular frame of reference. Unfortunately, often it is not feasible to carry out such experiments and one has to resort to using powder methods. It is worth emphasizing that each different NMR experiment weights the various NMR interactions differently, enabling one to obtain reliable overall results. Experiments carried out at different strengths of applied magnetic fields vary the relative contributions from chemical shift and coupling interactions. Although the magnitudes of R and J are independent of field, the observed splittings may depend on the magnetic field,[53] and of course on the type of spin system, *i.e.*, A_2 versus AX. Rapid sample spinning at the magic angle removes anisotropic interactions, so that isotropic chemical shifts and spin−spin coupling constants can be obtained. On the other hand, VAS scales anisotropic interactions so the relative contributions of isotropic and anisotropic interactions can be controlled. The 2D spin−echo experiment gives the spin−spin interactions in the F_1 domain and correlates the spin−spin interaction with the chemical shift interaction, providing valuable information on their relative orientations.

(51) (a) Raleigh, D. P.; Creuzet, F.; Das Gupta, S. K.; Levitt, M. H.; Griffin, R. G. *J. Am. Chem. Soc.* **1989**. *111*, 4502. (b) McDermott, A. E.; Creuzet, F.; Griffin, R. G. *Biochemistry* **1990**, *29*, 5767. (c) Creuzet, F.; McDermott, A.; Gerhard, R.; Van er Hoef, K.; Spijker-Assink, M. B.; Herzfeld, J.; Lugtenburg, J.; Levitt, M. H.; Griffin, R. G. *Science* **1991**, *251*, 783. (d) Peersen, O. B.; Yoshimura, S.; Hojo, H.; Aimonto, S.; Smith, S. O. *J. Am. Chem. Soc.* **1992**, *114*, 4332. (e) Peersen, O. B.; Smith, S. O. *Concepts Magn. Reson.* **1993**, *5*, 303. (f) Peersen, O. B.; Groesbeek, M.; Aimoto, S.; Smith, S. O. *J. Am. Chem. Soc.* **1995**, *117*, 7228. (g) Griffiths, J. M.; Ashburn, T. T.; Auger, M. A.; Costa, P. R.; Griffin, R. G.; Lansbury, P. T., Jr. *J. Am. Chem. Soc.* **1995**, *117*, 3539. (h) Raleigh, D. P.; Levitt, M. H.; Griffin, R. G. *Chem. Phys. Lett.* **1988**, *146*, 71.

(52) (a) Song, Z.; Antzutkin, O. N.; Feng, X.; Levitt, M. H. *Solid State Nucl. Magn. Reson.* **1993**, *2*, 143. (b) Antzutkin, O. N.; Song, Z.; Feng, X.; Levitt, M. H. *J. Chem. Phys.* **1994**, *100*, 130. (c) Raleigh, D. P.; Kolbert, A. C.; Griffin, R. G. *J. Magn. Reson.* **1990**, *89*, 1.

(53) (a) Chu, P. J.; Gerstein, B. C. *J. Chem. Phys.* **1989**, *91*, 2081. (b) Eichele, K.; Wasylishen, R. E. *J. Magn. Reson., Ser. A* **1994**, *106*, 46. (c) Eichele, K.; Lumsden, M. D.; Wasylishen, R. E. *J. Phys. Chem.* **1993**, *97*, 8909. (d) Wu, G.; Lumsden, M. D.; Ossenkamp, G. C.; Eichele, K.; Wasylishen, R. E. *J. Phys. Chem.* **1995**, *99*, 15806.

Finally, rotational-resonance experiments yield the effective dipolar coupling constant. Also, successful simulation of MAS line shapes obtained under conditions of rotational resonance provides an additional stringent test of the reliability of NMR parameters obtained through spectral analysis.

Once the spin system is properly analyzed, valuable structural information can be extracted. Provided the anisotropy of the indirect spin−spin interaction and molecular motion are negligible, the effective dipolar coupling constants can be used to obtain the internuclear separation. In favourable cases, where typical chemical shift tensor orientations of functional groups are known, the relative orientation of chemical shift tensors indicates the relative orientation of those groups. It is anticipated that the results presented here will serve as a benchmark for future first-principle theoretical calculations of phosphorus shielding tensors in transition metal complexes.

Acknowledgment. We thank Dr. James F. Britten for assistance with the single-crystal NMR study, Dr. Michael D. Lumsden for obtaining solution proton spectra, Dr. Boqin Q. Sun and Prof. Robert G. Griffin for a listing of the program NMRLAB. Also, we thank Prof. Malcolm H. Levitt and Prof. Aatto Laaksonen for the computer programs CC2X and CC2Z. We thank Dr. Xialong Feng for helpful discussions and for a listing of a pulse program for rotational-resonance measurements. We also acknowledge Dr. Gang Wu for advice, the Dalhousie solid-state NMR group for suggestions, and Katherine N. Robertson for assistance in processing the X-ray diffraction data. We are grateful to the Natural Sciences and Engineering Research Council (NSERC) of Canada for supporting this study through research, equipment and major installation access grants. REW is grateful to the Canada Council for a Killam Research Fellowship. All NMR spectra were obtained at the Atlantic Region Magnetic Resonance Centre, supported by NSERC of Canada.

Supporting Information Available: Listings of crystal data and structure refinement, atomic coordinates and isotropic displacement parameters, anisotropic displacement parameters, *U* values, and bond distances and angles (20 pages). Ordering information is given on any current masthead page.

IC9806232